

VALUE OF INFORMATION IN MULTI ATTRIBUTE DECISION MAKING FOR AUTONOMY

Sam Kassoumeh^a
skassoumeh@oakland.edu

Vijitashwa Pandey^a
pandey2@oakland.edu

David Gorsich^b
david.j.gorsich.civ@mail.mil

Paramsothy Jayakumar^b
paramsothy.jayakumar.civ@mail.mil

^a Industrial & Systems Engineering, Oakland University, Rochester, Michigan, USA 48309

^b US Army Combat Capabilities Development Command
Ground Vehicle Systems Center, 6501 E. 11 Mile Road, Warren, MI 48397

ABSTRACT

This work presents some results in the value of information calculations for multi-attribute decision making under uncertainty. Almost all engineering activities are undertaken in the face of uncertainty and a decision that maximizes a suitably chosen metric is generally selected. It becomes essential sometimes to collect information regarding these uncertainties so that better informed decisions can be made. Calculation of the worth of this information (*VoI*) is a difficult task, particularly when multiple attributes are present and there exists dependence between the random attributes in the same alternative or across different alternatives. In this paper, closed-form expressions and numerical models for the calculation of *VoI* are presented. Particularly, we derive methods for the general scenario where we have to decide over two or more alternatives, each involving two or more continuous random attributes exhibiting some level of dependence with the others. These reduce or completely eliminate the need for conducting simulations or approximations, both of which tend to be either computationally expensive (such as Monte Carlo), limited in accuracy or both. It also allows us to conduct more involved analyses such as sensitivity analysis on design parameters and the engineer's preferences in a feasible and even potentially automated way. We also introduce "attribute-wise *VoI*", which shows that collecting information on one or more of the attribute(s) makes sense only in specific dependence scenarios and tradeoff relationships between attributes. Calculation methods for value of such information are also provided. We illustrate our models on mobile autonomous system selection decisions. We conclude with a discussion on the avenues for future research into the optimal mix of a system's intelligence (autonomy), communication and information gathering.

KEYWORDS:

Value of information, multi-attribute decisions, uncertainty mitigation, risk aversion, autonomous vehicles

NOMENCLATURE

CE_i	Certainty Equivalent over the i th uncertain attribute
MCS	Monte Carlo simulation
MVN	Multivariate normal
RON	Range of negotiability
$\mathbb{E}[U(.)]$	Expected utility
EU_{error}	Allowed error in $\mathbb{E}[U(.)]$ before and after information when accounting for full <i>VoI</i>
K	Normalizing parameter to be used in the multilinear utility function.
n_{gen}	Number of random generations
R	Risk tolerance used in exponential utility functions
$U(.)$	Single attribute utility function
V	Value of information
VoI_{AWmin}	Minimum attribute-wise <i>VoI</i>
$f_X(x)$	Probability density function of a continuous random variable X
k_i	Scaling constant for the i th attribute
p	Probability of uncertain outcome
ρ_{XY}	Correlation between variables X and Y
Σ	Positive definite covariance matrix
$ \Sigma $	Determinant of Σ
$\Phi(x, \mu, \sigma)$	CDF of a Gaussian distribution

1. INTRODUCTION

Uncertainty is extremely prevalent in engineering design problems where one must select the best design(s) from a set of multiple options, each leading to uncertain attribute realizations. In this paper, similar to (Malak et al. 2009), we use the term "uncertainty" to characterize the "variability" representable using a probability density function. There are many techniques available in the literature to make design-decisions under uncertainty, such as, for robust design (Chen et al., 1996 and Mourelatos et al. 2006), reliability based design optimization (RBDO) (Choi et al., 2002 and Liang et al., 2007), and flexible

design (Cardin et al., 2008 and De Neufville, 2011). Concurrent work exists in uncertainty quantification and propagation, where extremely limited data is available or the calculation of the system outputs is computationally expensive (Nannapaneni et al. 2016). Clearly, there also exist situations where uncertainty is so large that it is best to delay the decision until the uncertainty has been resolved to some extent.

Alternatively, it also becomes possible in many practical design problems, to reduce uncertainty through collection of data or expert opinions. The immediate concern then becomes: how much information should be collected, or when translated into cost units, how much money should be expended to collect this additional information? This is termed Value of Information (*VoI*) in formal decision analysis. In general, the theory of the value of information is based on considering both, the uncertainties and its economic impact (Howard 1966). In other words, it involves finding the monetary value, additional to the cost of a particular design, of reducing or completely eliminating the uncertainty associated with it. When it is possible to eliminate the uncertainty completely, one can then calculate the value of *perfect* information. This is very beneficial in finding the maximum amount that someone should pay to completely eliminate the uncertainty associated with a specific option. In situations where the uncertainty is only reduced but not eliminated, the value of imperfect information is calculated (sometimes also called the expected value of sample information). This is useful in understanding the worth of conducting an experiment or simulation – which because of various constraints only reduce uncertainty. Prior efforts have looked into the benefits of value of information theory over wide range of applications including medical decisions, economics, environmental, energy, and increasingly in engineering design. Keisler et. al. (2014) gave an in-depth literature review on the applications trend of the *VoI*.

Decisions involving the selection of the correct vehicle platform for a specific application are challenging, particularly vehicles that are expected to perform in on-road as well as off-road environments. That is due to the uncertainties involved in the operating conditions and the performance of the vehicles themselves. The decision problems become more complex with the recent efforts to introduce autonomy and intelligence in these vehicles, as additional sources of uncertainty are involved. These include issues such as latency and bandwidth for tele-operated vehicles, and sensor fusion in fully autonomous vehicles. In this paper, we illustrate our models on mobile autonomous system selection decisions.

Generally, the complexity of the problem is a function of different attributes such as the number of possible outcomes or alternatives, the number of uncertainties and the level of knowledge about the characteristics of these uncertainties. For example, in medical decision making scenarios, the decision can be simply among three choices: treatment, no treatment and test, with two deterministic outcomes: healthy and unhealthy with their associated probabilities (Felder et al. 2017), while other decision problems can involve as many as 10 parameters, each with its own probability distribution (Strong et al. 2013 and

2014). Another example on using *VoI* in complex problems is looking into design decision scenarios of complex systems and how *VoI* can help in simplifying and optimizing the design process. For example, Panchal et. al. (2009) proposed a *VoI* metric called “improvement potential” to compare among the different design alternatives. *VoI* studies have also shown interesting results on the effect of uncertainty reduction on the risk attitude of the decision maker. For example, Wijayarathna and Dixit (2016) found that providing information early in a route selection scenario, where delay time was the only decision attribute, can change the risk attitude of the decision maker, particularly reducing risk aversion and also, not necessarily causally, the *VoI*. Another example of complex systems engineering problems is geotechnical projects, such as tunnels, where uncertainties play a major role in decision making (Xia et al. 2017).

Whereas prior research has looked into the value of information methodology and applied it to a range of applications, the majority of methods surveyed have utilized concepts such as expected value, project value or net benefit of an outcome, as opposed to a utility function as the formal decision theoretic method requires. For example, Strong et. al.(2013 and 2014) found an efficient method to overcome two of the drawbacks, high computation cost and inefficiency when the input parameters are correlated, for Monte Carlo simulations in calculating *VoI*, the main function for calculating *VoI* was found using the *net benefit* function. While the approach is interesting, the results may not be generalizable to a wider class of utility functions and distributions. Using a utility function is beneficial in capturing the risk-attitude of the decision maker and influences the decision making process including *VoI* calculations.

Expectedly, using utility functions directly in *VoI* analysis is not without challenges and we address some of them here in this work. We also extend the analytical and numerical models to problems involving multiple attributes. We provide $E[U(.)]$ and *VoI* expressions for the multilinear form of the utility function for two or more attribute problems. The utility independence required for the use of the multilinear form allows us to generalize the *VoI* from results acquired in the single attribute cases. While the advancements in computational power and methods have allowed the modeling and simulation of increasingly complex problems, it is still preferable to be able to evaluate analytical or efficient numerical expressions without the need for expensive simulations. Furthermore, availability of these results also allows us to perform sensitivity analysis in a straightforward fashion.

This paper is organized as follows. In the next section, expressions and methods for $E[U(.)]$ and *VoI* for multi-attribute problems are presented. Next we summarize the main factors affecting *VoI*. Results and discussion will follow as we apply the new methods on some notional case studies involving selection decision between vehicles that exhibit some level of autonomy. Last section will present conclusions and propose future work.

2. MULTI-ATTRIBUTE MULTI-LINEAR UTILITY FUNCTION

A significant majority of design-decision problems in engineering involve multiple attributes. In such cases, one not only needs to model single attribute preferences, one must also understand the tradeoff behavior of the decision maker in addition to their multi-attribute preferences over risk. Arguably, they constitute a non-trivial and at the same time essential extensions of single attribute decision problems.

We use the multilinear, multiattribute utility function (MAUF) (Keeney 1977 and Keeney and Raiffa 1993) to measure utility over multiple attributes and we provide a brief overview here. This choice is incident from the tractability the function affords in modeling the preferences of a decision maker, in addition to being flexible enough to model a wide range of preference structures. One first selects a range of negotiability (RON) for each attribute, which provides the upper and lower bounds on an attribute. This is important in multiattribute problems to limit our analysis to feasible and realistic situations and to provide clarity in decision making. Let the attributes form the vector $X = (X_1, \dots, X_n)^T$ or its realization $(x_1, \dots, x_n)^T$. The multilinear utility functional form is given by:

$$U(x_1, \dots, x_n) = \frac{1}{K} \left[\prod_{i=1}^n (Kk_i U_i(x_i) + 1) - 1 \right] \quad (1)$$

This functional form is widely used because it allows the utility functions to be defined over individual attributes separately. Each single attribute utility function, $U_i(X_i)$ is a utility function over the attribute X_i and takes a value of 1 if the attribute is at the best possible level, and 0 if the attribute is at the worst possible level within its range of negotiability. The exponential form of the single attribute utility function with range of negotiability becomes:

$$U_x(x_i) = \frac{1 - e^{-\frac{(x_{\max} - x_i)}{R_x}}}{1 - e^{-\frac{(x_{\max} - x_{\min})}{R_x}}}, \text{ when less of the attribute is better}$$

$$U_x(x_i) = \frac{1 - e^{-\frac{(x_i - x_{\min})}{R_x}}}{1 - e^{-\frac{(x_{\max} - x_{\min})}{R_x}}}, \text{ when more of the attribute is better}$$

Consequently, from the very construction of the utility function, if $U = 1$, one has attained the best level on all attributes simultaneously and if $U = 0$, one has attained the worst values on all attributes simultaneously. The scaling constants, k_i , measure the relative disinclination of the decision maker to trade off the i th attribute for improvement in other attributes. The individual utility functions and the scaling constants are assessed using standard lottery techniques described in the literature (Nikolaïdis et al. 2011). The normalizing parameter, K , is calculated by setting all the single attribute utilities as well as the multi-attribute utility equal to 1 in Equation (1) and solving for K .

In order for us to construct the functional form in Equation (1) above from single attributes, we should first check that the

attributes exhibit preferential and utility independence. Preferential independence implies that the decision maker has the same preference order over an attribute when the other attributes are fixed, everywhere in the attribute space. An example is when a designer is considering beam designs over two attributes: strength and cost. Most designers will likely prefer a stronger beam to a weaker one, regardless of where the cost attribute is fixed. And vice versa for cost to strength. Utility independence implies that the certainty equivalent corresponding to an attribute is independent of where the other attributes are fixed. Utility independence implies preferential independence. The functional form used in Equation (1), implies and is implied by the utility independence condition.

3. DERIVATION OF $\mathbb{E}[U(\cdot)]$ AND $V\sigma I$ IN MULTI ATTRIBUTE SCENARIO

3.1. Two attribute decision problem with one random attribute.

We start with two attribute decisions, where one attribute is deterministic and the other is a random variable following Gaussian distribution. Consider the decision problem shown in figure 1, involving a choice between two options, A and B. Option A is uncertain over the attribute X and $f_{X_A}(x_A) \sim N(\mu_{x_A}, \sigma_{x_A}^2)$. In this scenario, closed form expressions can be found for both: $\mathbb{E}[U(\cdot)]$ for the random alternative, as well as the $V\sigma I$ for the decision.

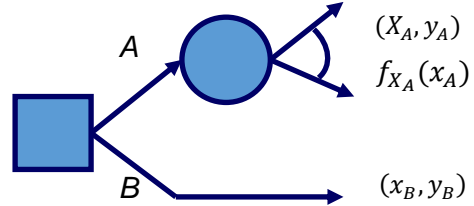


Figure 1. A two-attribute decision with one uncertain alternative.

To find the expected utility of option (A), we use the MAUF from Equation (1), which can be written for two attributes as:

$$U(x, y) = \frac{1}{K} [(Kk_x U_x(x) + 1)(Kk_y U_y(y) + 1) - 1] \quad (2)$$

So we find:

$$\begin{aligned} \mathbb{E}[U(A)] &= \int_{-\infty}^{\infty} U(x, y) f_X(x) dx \\ &= \int_{-\infty}^{\infty} U(x, y) \left(\frac{1}{\sigma\sqrt{2\pi}} e^{-\frac{(x-\mu)^2}{2\sigma^2}} \right) dx \end{aligned}$$

We evaluate the integral and find the resulting expression in Table (1). Notice that the expectation of the utility of a simple scenario of one attribute following Gaussian distribution has been known since the work of Howard (1971). Also, the $V\sigma I$ expressions the analysis for single attribute were found by Bickel (2008), Delique (2008), Zan and Bickel (2013) and Sun and Abbas (2014), here we extend these results to the multi-attribute

scenario shown in Figure (1). In order to calculate for the VoI , we need first to understand the ranges for the random variable X that make the $\mathbb{E}[U(A)] > U(B)$ and vice versa. We consider the use of “certainty equivalent” CE_x : the certainty equivalent over the uncertain attribute. This is the sure amount that makes a decision maker indifferent between a sure outcome with $(x_A = CE_x, y_A)$ on one hand, and option (B) on the other. When the random variable X in option A is less than that amount, and if we consider the smaller of that attribute the better, then $\mathbb{E}[U(A)] > U(B)$ and vice versa. That deterministic amount is found by equating:

$$MAUF_A = U(B) \quad (3)$$

$$\frac{1}{K} \left[(Kk_x U_x(x_A) + 1) (Kk_y U_y(y_A)) - 1 \right] = U(B) \quad (4)$$

Where:

$$U_x(x_A) = \frac{1 - e^{-\frac{(x_{max} - CE_x)}{R_x}}}{1 - e^{-\frac{(x_{max} - x_{min})}{R_x}}} = \frac{1 - e^{-\frac{(x_{max} - CE_x)}{R_x}}}{D_x} \quad (5)$$

$$U_y(y_A) = \frac{1 - e^{-\frac{(y_{max} - y_A)}{R_y}}}{1 - e^{-\frac{(y_{max} - y_{min})}{R_y}}} = \frac{1 - e^{-\frac{(y_{max} - y_A)}{R_y}}}{D_y} \quad (6)$$

We substitute (6) and (5) in (4) and solve for CE_x

$$CE_x = R_x \log_e \left[1 - \frac{(\frac{ab}{c} - 1) D_x}{Kk_x} \right] + x_{max} \quad (7)$$

Where:

$$a = Kk_x U_x(x_B) + 1, \quad b = Kk_y U_y(y_B) + 1$$

$$c = Kk_y U_y(y_A) + 1$$

Now we can find the VoI , similar to Equation (5):

$$\mathbb{E}[U(V)] = \int_{-\infty}^{CE_x} MAUF(A, V) f_X(x) dx + \int_{CE_x}^{+\infty} MAUF(B, V) f_X(x) dx \quad (8)$$

We evaluate and solve for V , the closed-form solution is shown in Table (1).

Table 1: Expected utility and Value of Information expressions for two attributes utility function and one uncertainty follows a Gaussian distribution

$\mathbb{E}[U(A)] = \frac{1}{K} \left[(Kk_y U_y(y) + 1) * \left(Kk_x \frac{1 - e^{-\frac{(x_{max} - x_{min})}{R_x}}}{1 - e^{-\frac{(x_{max} - \mu_x)}{R_x}}} + 1 \right) - 1 \right]$	
$V = R_y \ln \left[\frac{\frac{k_y}{D_y} \beta + \frac{(1 - \Phi(CE_x, \mu_x, \sigma_x))}{K} \left[(Kk_x U_x(x_B) + 1) \left(\frac{Kk_y}{D_y} + 1 \right) - 1 \right] + \frac{k_x}{D_x} \alpha - \max(\mathbb{E}[U(A)], U(B))}{k_y \left(\frac{1}{D_y} - U_y(y_B) \right) + (1 - \Phi(CE_x, \mu_x, \sigma_x)) \left[(Kk_x U_x(x_B) + 1) k_y \left(\frac{1}{D_y} - U_y(y_B) \right) \right]} \right]$	
Where:	
<p>➤ CE_x: The certainty equivalent over the uncertain attribute. This is the sure amount that makes a decision maker indifferent between a sure outcome with $(x_A = CE_x, y = y_A)$ on one hand, and the outcome in option (B) where $(x = x_B, y = y_B)$ on the other hand.</p>	
<p>➤ $D_y = 1 - e^{-\frac{(y_{max} - y_{min})}{R_y}}, D_x = 1 - e^{-\frac{(x_{max} - x_{min})}{R_x}}, \beta = \frac{Kk_x}{D_{px}} \alpha + \Phi(CE_x, \mu_x, \sigma_x)$</p>	
<p>➤ $\alpha = \Phi(CE_x, \mu_x, \sigma_x) - e^{-\frac{\sigma^2 - 2R_x(x_{max} - \mu_x)}{2R_x^2}} \Phi\left(CE_x, \left(\mu_x + \frac{\sigma_x^2}{R_x}\right), \sigma_x\right)$</p>	

Note that the solution for the case when more of the attribute is better is exactly the same form but we substitute $(x_{max} - \mu_x)$ with $(\mu_x - x_{min})$. Furthermore, a non-Gaussian distribution for the random variables can be modeled as a mixture of Gaussians and provides a relatively straightforward extension of this result.

3.2. Decisions involving two or more correlated random variables

In this section, we generalize our method from the previous section into the more general decision scenarios with two or more random variables that exhibit some degree of statistical relationship (correlation). Correlation can exist not

only between attributes in the same alternative, but also between attributes across different alternatives. Calculations of $\mathbb{E}[U(.)]$ and VoI in this case not only reflect the more general and realistic engineering decision, but also have implications and insights on the optimal information gathering in a given scenario, since collecting information on one random variable can provide some information on the others. We show in Figure (2) a two-action notional example of this case, involving a decision scenario between two vehicles, A and B, where vehicle A exhibits uncertain performance over attributes X and Y , which are jointly distributed random variables following bivariate normal distribution. The density of this distribution is shown in Equation (9).

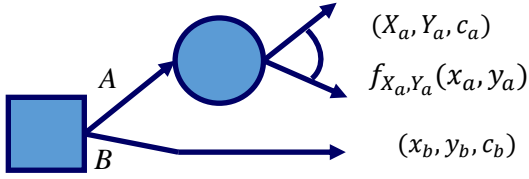


Figure 2. Decision with three attributes involving two correlated random variables.

Now, in order to calculate $\mathbb{E}[U(A)]$, we need to evaluate the expression in Equation (10), where $U(A)$ here is similar to the form in Equation (2), but we add another term for the attribute c , which is assumed a constant. In many engineering acquisition decisions, the attribute of cost exhibits this behavior – while other performance attributes may be uncertain, a decision maker generally knows how much an option costs. Nevertheless, the approach presented here can easily accommodate uncertainty in all the variables.

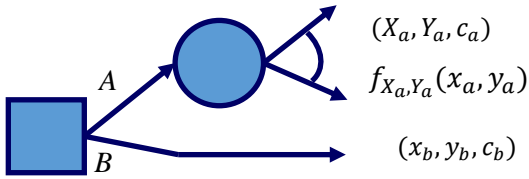


Figure 2. Decision tree for decision with three attributes, two are correlated random variables

$$f_{X,Y}(x,y) = \frac{1}{2\pi\sigma_X\sigma_Y\sqrt{1-\rho^2}} \exp\left(\frac{-1}{2(1-\rho^2)}\left(\frac{(x-\mu_X)^2}{\sigma_X^2} + \frac{(y-\mu_Y)^2}{\sigma_Y^2} - \frac{2\rho(x-\mu_X)(y-\mu_Y)}{\sigma_X\sigma_Y}\right)\right) \quad (9)$$

$$\mathbb{E}[U(A)] = \iint_{-\infty}^{+\infty} U(x,y,c) f_{X,Y}(x,y) dx dy \quad (10)$$

Where: ρ = correlation coefficient, which is a measure of the linear relationship between the two variables and is given by Equation (19) (Navidi, 2015).

$$\rho_{X,Y} = \frac{\text{Cov}(X,Y)}{\sigma_X\sigma_Y} \quad (11)$$

To our knowledge, no closed form solution exists for Equation (10). Therefore, MCS and efficient numerical method are proposed in the next sections.

3.2.1. Monte Carlo Simulation Methods to Calculate $\mathbb{E}[U(\cdot)]$ in the General Case:

For the rest of the paper, we consider a notional decision problem of selecting between two vehicles or vehicle platforms – essentially similar to the decision tree in Figure (2). The decision maker needs to select between two vehicles, A and B, over the following attributes:

1. Time to traverse a given terrain: (X) The preference order is ‘less is better’ and the range of negotiability, $\text{RON} = [45\text{s}, 180\text{s}]$, where: $X_a \sim N(100, (10)^2)$, $x_b = 100$ s.
2. Trafficable Percent Area, TPA: (Y) which is the percentage of the area of a given terrain that is trafficable by a vehicle, without getting stuck by an obstacle, uneven surface or other similar terrain related properties. The preference order is ‘more is better’ and the range of negotiability, $\text{RON} = [10\%, 100\%]$, where: $Y_a \sim N(0.65, (0.20)^2)$, $y_b = 0.6$.
3. Total Cost: (c), The preference order is ‘less is better’ and the range of negotiability, $\text{RON} = [\$100\text{k}, \$1,000\text{k}]$, where: $c_a = c_b = \$400\text{k}$.

Let us also assume that the decision maker has chosen, for this particular decision scenario, the following risk tolerance values and scaling constants. Note that, the method is dependent on the choice of these parameters:

$$R_x = 90, R_y = 0.5, R_c = 400 \\ k_x = 0.2, k_y = 0.3, k_c = 0.1$$

We will be analyzing the sensitivity of $\mathbb{E}[U(A)]$ over the range of ρ : $-1 \leq \rho \leq +1$.

To benchmark the numerical method, we first use the algorithm shown in Figure (3) to calculate expected utility for the uncertain alternative A using monte carlo simulation (MCS). The total number of generations (n_{gen}) that is required in step 1 of the algorithm is set to: $n_{gen} = 10^7$. Figure (4) show the effect on $\mathbb{E}[U(A)]$ of change in ρ .

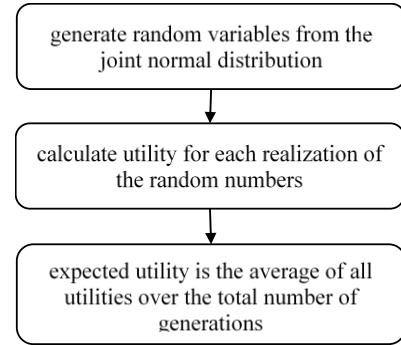


Figure 3. MCS algorithm for calculating $\mathbb{E}[U(A)]$ for an alternative with jointly distributed normal random variables

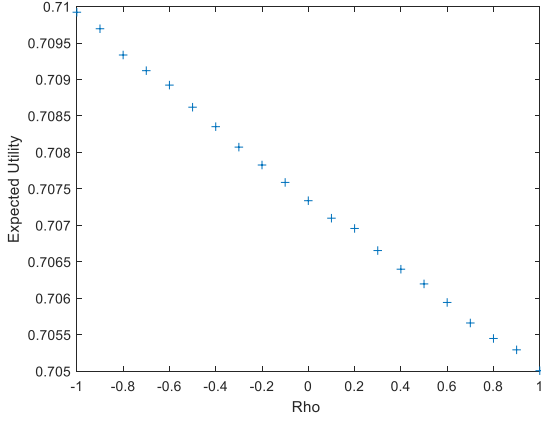


Figure 4. Expected utility against ρ for vehicle A from Figure (2) using MCS when $n_{gen}=10^7$

By examining the results in Figure (4) we notice that expected utility has approximately linear trend when plotted against different ρ values, everything else being constant. This trend is more evident, the higher the value of n_{gen} . The decreasing trend of $\mathbb{E}[U(A)]$ is due to both random attributes (X and Y) having opposite preference order, recall that X is less-is-better and Y is more-is-better type. The trend becomes an increasing one when both attributes have the same preference order. This is easily verified by reversing one of the attributes' preference in the MAUF (Equation (1)).

3.2.2. Numerical method to calculate $\mathbb{E}[U(\cdot)]$ in the general case.

Prior research has extensively studied the problem of evaluating or estimating multiple integrals when dealing with multivariate normal (MVN) distribution with correlated variables. Different methods are used in the literature to achieve this goal including series expansion methods, such as: tetrachoric series for the bivariate case by Pearson (1901), Taylor Series expansion by Olson and Weissfeld (1991) to approximate the multivariate case, a novel series expansion based on Fourier Series by Fayed and Atiya (2014). Some approximation methods looked into approximating the multinormal integral by a product of one-dimensional normal integrals (Pandey, 1998). Another method by (Miwa et al. 2003) used recursive integration algorithm to evaluate non-centered probabilities. Some work has even looked at the general case where the random variables do not follow MVN, rather to solve multi integrals of any jointly random variables using numerical integration (Zhou and Nowak, 1988).

One method that is frequently used and cited in the literature as being robust and efficient method is the Gaussian Quadrature. For example, the computation of the bivariate normal integral was studied by Drezner (1978) and later by Drezner and Wsolowsky (1990) using the Gaussian quadrature method. Genz (1992, 1993 and 2004) later presented a modified form of that algorithm for the bivariate and tri-variate normal probabilities for rectangles using numerical integration. Further improvements to Genz method was also performed by Brodtkorb (2006), where they used regression to eliminate low probability regions and developed a new method to determine

redundant variables for faster estimates. Also, Somerville (1998) presented Fortran 90 algorithms to numerically calculate the multivariate normal and multivariate-t probabilities over convex regions instead of rectangles, where their method also relied on the Gauss-Legendre quadrature to estimate the value of the integral.

In general, most of the methods surveyed were used for calculating MVN probabilities, and we did not find them flexible enough to calculate expectations of utility. Also, each had some drawbacks in application. For example, Taylor series performs poorly at levels of ρ close to 0.9 (Olson & Weissfeld, 1991). Moreover, most approximation methods rely on numerical integration after reducing the number of random variables in the problem to around 5. Therefore, we selected the Gaussian quadrature method with numerical integration for its efficiency and flexibility of evaluating integrands with relatively low dimension. This is acceptable in our case because the general rule of thumb for the number of attributes in a multi-attribute decision scenario is between 2 and 5. Also, from a practical standpoint, the work by Shampine (2008) has resulted in an improved method (in MATLAB) based on function vectorization for faster and more reliable results.

To apply the numerical method to finding $\mathbb{E}[U(\cdot)]$ for correlated random variables, we consider the decision problem in Figure (2), where we need to calculate expected utility for random alternative A, $\mathbb{E}[U(A)]$. We evaluate Equation (10) as follows:

$$\mathbb{E}[U(A)] = \int_{-\infty}^{+\infty} \int_{-\infty}^{+\infty} \{MAUF\} \{pdf\} dx dy \quad (12)$$

Using Equation (1) for MAUF for three attributes, we find:

$$\begin{aligned} \mathbb{E}[U(A)] = \int_{-\infty}^{+\infty} \int_{-\infty}^{+\infty} \frac{1}{K} [(Kk_x U(X_a) + 1)(Kk_y U(Y_a) \\ + 1)(Kk_c U(c_a) + 1) - 1] \\ * pdf dx dy \end{aligned} \quad (13)$$

Since the cost attribute (c_a) here is deterministic:

$$\begin{aligned} = \frac{(Kk_c U(c_a) + 1)}{K} * \int_{-\infty}^{+\infty} \int_{-\infty}^{+\infty} [(Kk_x U(X_a) + 1)(Kk_y U(Y_a) \\ + 1)] pdf dx dy - \frac{1}{K} \int_{-\infty}^{+\infty} \int_{-\infty}^{+\infty} pdf dx dy \end{aligned} \quad (14)$$

But we know that: $\int_{-\infty}^{+\infty} \int_{-\infty}^{+\infty} pdf dx dy = 1$

Also, let (Q) be the result of numerical evaluation of the double integral, we then find:

$$\mathbb{E}[U(A)] = \left[\left(kc U(c_a) + \frac{1}{K} \right) * Q \right] - \frac{1}{K} \quad (15)$$

Where:

$$Q = \int_{-\infty}^{+\infty} \int_{-\infty}^{+\infty} [(Kk_x U(X_a) + 1)(Kk_y U(Y_a) + 1)] pdf dx dy \quad (16)$$

The method in Equation (15) requires only one evaluation of the numerical integral (Q), which on average requires around 0.01 seconds of computational time on a personal laptop computer, with Intel processor of 2.9 GHz speed and 4GB of memory. The advantage of writing the model in the form in Equation (15) is to show the simplicity in scaling the model

into 3 or more attributes problems, we only add SAU term in Equation (16) for each additional random variable, and use the correct MVN pdf accordingly. In the next section, we compare this method with MCS in calculating expected utility.

Comparison between Numerical and MCS method for $\mathbb{E}[U(.)]$

We now use our numerical method in Equations (15) and (16) to calculate $\mathbb{E}[U(A)]$ as a function of ρ , the results are shown in Figure (5). We notice that we get almost identical results with the numerical method to the ones found in Figure (4) using MCS. Table (2) show a comparison of the results for selected ρ values. Not only the linear trend is more evident in the numerical method than the MCS method, the computational time required in the numerical method was 3.4 seconds only, compared to 12 seconds using MCS.

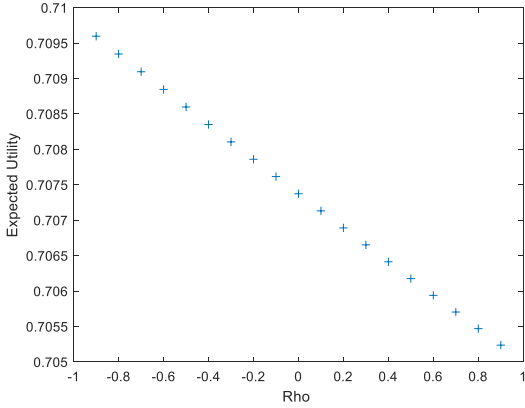


Figure 5. Expected utility against ρ for vehicle A from Figure (2) using the numerical method

Table 2: Comparison between EU_{MCS} and $EU_{Numerical}$ methods in 3 attributes over selected ρ values

ρ	-0.9	-0.5	0	+0.5	+0.9
$EU_{Numerical}$	0.70960	0.70860	0.70737	0.70618	0.70524
EU_{MCS}	0.70960	0.70857	0.70744	0.70620	0.70528

We now generalize the numerical method by considering an n -dimensional Gaussian distribution given in Equation (17) (Gill, 2014).

$$N_n(\mathbf{X}|\boldsymbol{\mu}, \boldsymbol{\Sigma}^2) = (2\pi)^{-\frac{n}{2}} |\boldsymbol{\Sigma}|^{-\frac{1}{2}} \exp \left[-\frac{1}{2} (\mathbf{X} - \boldsymbol{\mu})' \boldsymbol{\Sigma}^{-1} (\mathbf{X} - \boldsymbol{\mu}) \right] \quad (17)$$

Where:

\mathbf{X} is n -dimensional vector of variables

$\boldsymbol{\mu}$ is the corresponding n -dimensional means vector

$\boldsymbol{\Sigma}$ is the $n \times n$ -dimensional, positive definite covariance matrix

$|\boldsymbol{\Sigma}|$ is the determinant of $\boldsymbol{\Sigma}$

Consider now a decision problem shown in Figure (6). This decision problem is very similar to the previous decision problem, except we add a fourth attribute which is *latency* - a measure of the communication delay encountered with a

vehicle that exhibits some level of autonomy, such as tele-operated vehicles or full autonomous vehicles with sensing feed. Let us assume that latency (L) is a random variable that follows a normal distribution and is correlated with the other attributes of time and trafficable percent area. Additionally, it is also a decision attribute with its own range of negotiability. The relevant parameters are listed below.

$$L \sim N(0.7, (0.20)^2), R_l = 0.9, k_l = 0.2, RON = [0s, 2s] \quad . \\ \rho_{XL} = +0.5, \rho_{YL} = +0.7.$$

To preserve the positive definiteness of the covariance matrix of the random variables and to avoid numerical issues arising out of using a correlation value very close to one, ρ_{XY} in this scenario only ranges between: $-0.2 \leq \rho_{XY} \leq +0.9$.

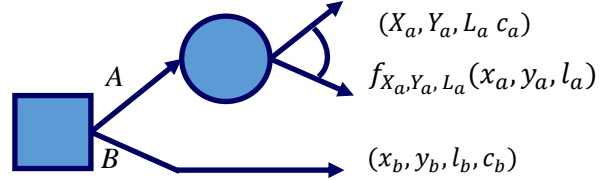


Figure 6. Decision tree for decision with four attributes, three are correlated random variables

The time required to evaluate the expected utility in this case with four attributes was 3.2 seconds. This time would have increased to around 5 seconds if it were feasible to calculate over 19 values of ρ_{XY} as we did in the case of three attributes. This confirms that computational time is still manageable as we scale our method to higher number of attributes. The time required to do the same analysis using MCS method was 10.8 seconds. While the improvement in computational time is evident in the case when calculating expected utility using our numerical method, we will show in the next sections that the substantial advantage in computational time is more evident when calculating *VoI*.

3.2.3. Monte Carlo simulation to calculate *VoI* in the general multiattribute case

We show use an MCS method to estimate the *VoI* for the same example in Figure (2). It is worth mentioning that while the method here is shown for notional example with 2 alternatives where one is random, it can easily be modified to calculate *VoI* for decision scenarios with both alternatives are random, or for scenarios with three or more alternatives. To calculate the *VoI*, we find the amount that satisfies Equation (18). Practically, we allow small error in Equation (18) that we call “ EU_{error} ” under which the error in the resulting *VoI* calculation will be negligible. The overall MCS algorithm is shown in Figure (A.1) in the Appendix. Clearly, the first step in the algorithm is the same as the algorithm found in the prior section for calculating expected utility without information.

$$\mathbb{E}[U_{without\ info}] = \mathbb{E}[U_{with\ info}] \quad (18)$$

We notice from analyzing the algorithm that the required time to calculate VoI is very large compared to only calculating expected utility. Clearly, using a simple linear search to find the correct V will be very computationally intensive. For example, when we use $n_{gen} = 10^4$ over $-1 \leq \rho \leq +1$ range, total time required is 2,663 seconds (~ 45 minutes). Therefore, we use binary search method instead of linear search to find V , which reduces the search complexity from $O(n)$ to $O(\log n)$ (Seidl et al, 2011).

Using the proposed algorithm we can now calculate the VoI more efficiently, for example, for $n_{gen} = 10^7$ the time required was 178 seconds. Clearly the smaller the allowed error in expected utility, the more accurate the results for VoI . Therefore, the results emphasize the high level of accuracy required in expected utilities calculations, specifically for VoI calculations purposes. Another major observation we notice from Figure (7) is the relatively wide range of VoI across the range of ρ values. This shows the large impact of the correlation coefficient (ρ) on VoI . Therefore, assuming independence between random variables, especially when finding VoI over one or a subset only of the variables, can lead to erroneous results.

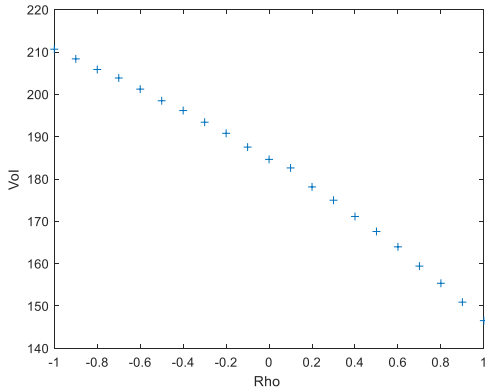


Figure 7. VoI against ρ when $n_{gen} = 10^7$, $EU_{error} = 10^{-5}$ using MCS with binary search

3.2.4. Numerical calculation of VoI in the general multiattribute case

We will focus in this section on deriving an efficient method for calculating VoI in scenarios where information is collected on all the attributes, which we call “Full-attribute VoI ”. In a later section, we will discuss the scenarios when we collect information on only a subgroup of the random variables, and see how the model and results will change.

Problems in two or more dimensions

Let us revisit the example in Figure (2), where we have three attributes in each alternative, two of the attributes in alternative A are random variables (X and Y). Here, with alternative B being deterministic as x_a and y_a are constants, we know that its utility is constant (regardless of the realizations of X_a and Y_a). In this case, we can draw its iso-preference curve as shown in Figure (8). An iso-preference curve is a collection of (x, y)

points that all have the same utility. Therefore, any realization of the pair (x_a, y_a) that is to the left of the iso-preference curve for B will mean that $\mathbb{E}[U(A)] > U(B)$, and vice versa. Notice, in this particular case, that the utopia point is at the minimum value of each attribute (from the range of negotiability), reflecting a less-is-better preference order for both attributes. Now, since in our example attribute Y has more-is-better preference, then a simple conversion is required to make it calculated as a less-is-better attribute. This can be easily accomplished by replacing each Y by $y_{max} + y_{min} - Y$. Each time we collect “full-attribute” information on X_A and Y_A , we can immediately decide whether $\mathbb{E}[U(A)] > U(B)$ or $\mathbb{E}[U(A)] < U(B)$ or $\mathbb{E}[U(A)] = U(B)$. More specifically, $\mathbb{E}[U(A)] > U(B)$ when the pair (x_a, y_a) is within the region (D). The expression for the isopreference curve is given by:

$$g_{iso}(x) = y_{max} + \left[R_y * \ln \left(1 + \frac{D_y}{K * k_y} - \frac{D_{y(1+K*EU_b)}}{(Kk_x U(x)+1)*(Kk_c U(c_a)+1)*K*k_y} \right) \right] \quad (19)$$

Therefore, using the density for the bivariate normal distribution, we can calculate the expectation for when (x_a, y_a) is inside or outside the region D, which is required to calculate the expected utility of the decision tree after receiving the full-attribute information. This concept can be extended into scenarios with three or more random variables. For example, in the case with 4 attributes decisions where each alternative has 3 random variables (X, Y, Z), the iso-preference curves become surfaces, where any (x, y, z) point that is inside that surface and closer to the utopia point (making sure all attributes have less-is-better preference order) will have higher expected utility than points outside that surface, and vice versa.

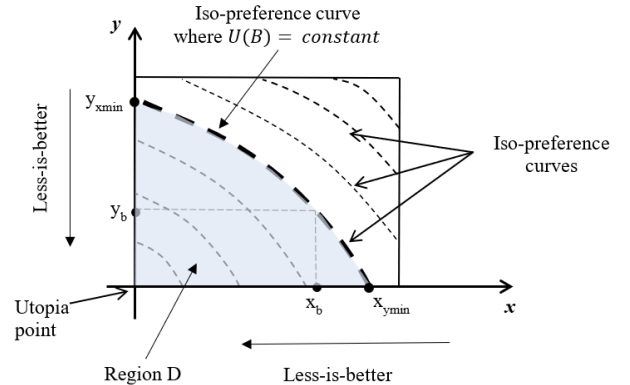


Figure 8. Iso-preference curve for $U(B)$ as a sure outcome and region D (highlighted) with higher utility

VoI in scenarios with one random alternative

We follow now the same steps in sections 2 and 4 to derive VoI : The detailed steps to derive VoI are shown in the Appendix.

$$V = R_c * \ln \left[\frac{\left[\left(\frac{Kk_c}{Dc} + 1 \right) (Q_2 + \gamma_b - \gamma_b Q_1) \right] - (K * MaxEU) - 1}{\left[Q_2 \left(\frac{Kk_c}{Dc} \right) e^{-\frac{(cmax-ca)}{R_c}} \right] + \left[(\gamma_b - \gamma_b Q_1) \left(\left(\frac{Kk_c}{Dc} \right) e^{-\frac{(cmax-ca)}{R_c}} \right) \right]} \right] \quad (20)$$

Equation (20) provides a model to calculate VoI for two action decisions where one is random and another leads to a deterministic outcome.

VoI results compared to Monte Carlo simulation method

We compare the results found using the model in Equation (20) to the results found using MCS (shown in Figure (7)). The results are shown in Figure (9). The computational time required to create the graph was only 0.6 seconds. That is compared to 178 seconds required for the MCS method. This confirms the large improvement in computational time required when using our numerical method. Also, the accuracy of this method is superior to the MCS method with any $EU_{error} \leq 10^4$. As mentioned earlier, the extension of this method to decision scenarios of 3 or more random variables is straightforward. We can modify the joint density function and the γ_a, γ_b variables to accept the additional random variables, and evaluate the higher dimensional integrals numerically.

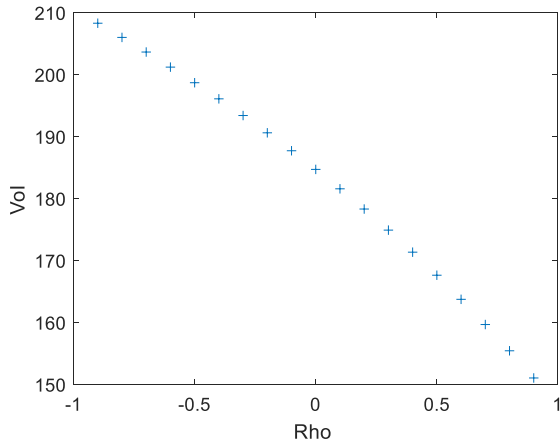


Figure 9. VoI against ρ using the proposed numerical method

3.2.5. Numerical method to calculate “attribute-wise VoI ” in the general case

In this section, we consider the VoI for situations where we collect information on only a subgroup of the random variables, whether it is a 2-action scenario with only one random alternative, or a scenario with two or more random alternatives, where alternatives exhibit some correlation among their variables. We call VoI in this case “attribute-wise VoI ”. While prior research have looked at correlated outcomes and/or more than 2-outcome decisions, such as Frazier and Powell (2010), Evangelou and Eidsvik (2016), Capser and Nikolaidis (2017), those efforts did not study the formal and more general case of multiattribute utilities and when the decision maker is risk averse.

We consider Figure (2) where only alternative A is random. Let us assume we are interested in finding VoI when collecting information on attribute X only. Clearly, collecting information on X can provide insights on the value of Y , since both are correlated. Calculation steps for expected utilities before information is the same as we did earlier and we can use the new numerical method for that step. To calculate VoI , we will follow similar algorithm to the one in Figure (A.1) in the appendix but with the following modifications:

1. We first only generate random realizations for one attribute, which are generated from its marginal pdf .
2. We calculate the conditional mean and standard deviation for Y , for each generated x_i , given by (Devore, 2012):

$$\mu_{y|x_i} = \mu_y + \frac{\sigma_y}{\sigma_x} \rho_{xy} (x_i - \mu_x)$$

$$\sigma_{y|x_i}^2 = (1 - \rho_{xy}^2) \sigma_y^2$$

3. Use the expression in Table (2) to find $EU_{after\ info}$ where one attribute is random, which in this case is Y , for each generated x_i .
4. Continue similarly as we did earlier to find VoI .

The results for the attribute-wise VoI , when we collect information on X only in the example in Figure (2), are shown in Figure (10), we have also added the full-attribute VoI results on the graph for comparison. The computational time required was 14.9 seconds. We notice that attribute-wise VoI here decreases to the lowest value at a specific value for $\rho_{xy} \approx 0.3$, before increasing again. That minimum VoI value is around 9.3, which is compared to full-attribute $VoI = 174.9$ at the same value of ρ_{xy} . That means for this specific decision scenario, when $\rho_{xy} \approx 0.3$, we will not gain much utility from collecting information only on attribute X . This result has very important implications on design and on strategies for collecting information. Another interesting result is that: $VoI_{\rho=0} > VoI_{\rho=0.3}$, for this particular scenario. This is interesting because it implies that for every decision scenario, there exists a value of the correlation coefficient that provides the lowest attribute-wise information which, counterintuitively, is not necessarily the point when $\rho_{xy} = 0$.

We also will find that VoI is very close at the extreme ends for $\rho_{xy} \approx \pm 1$ (i.e. perfect positive and perfect negative correlation). This is somewhat expected as information on one attribute should give more information on the other when their correlation is higher in absolute terms.

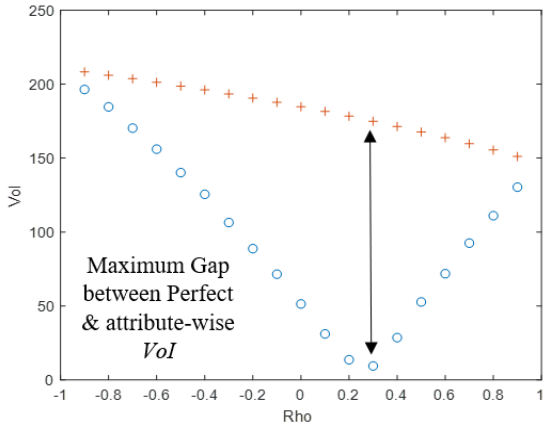


Figure 10. Full-attribute Vol (+) compared to attribute-wise Vol (o) for example in Figure (2), calculated against ρ .

We should also note that the non-monotonic trend in attribute-wise Vol is not always the case for all input parameters and constants. For example, if we increase σ_x from 10 to 30 and decrease σ_y from 0.2 to 0.1, then the same attribute-wise Vol trend when collecting info on X becomes monotonic and decreasing. We explain this by the fact that now more variation is attributed to X rather than Y , compared to the previous case. Therefore, collecting information over X , regardless of the correlation between X and Y will still be valuable to make better decisions.

All alternatives random and correlated:

In this section, we consider the more general case where we have two or more correlated random alternatives, and we are collecting information on a subgroup from the full vector of random variables (\mathbf{Z}). An example is shown in Figure (11). While we show here an example of two random alternatives, each with two random attributes, the extension to higher number of alternatives and random attributes is straightforward using the same methodology, as we will see in a case study later. Let us assume the decision maker is selecting between two autonomous vehicles, 1 and 2, each with random performance, where the variables have a joint multivariate normal distribution as follows. Let \mathbf{Z} be a vector of the random variables where:

$$\mathbf{Z} = \begin{bmatrix} X_1 \\ X_2 \\ Y_1 \\ Y_2 \end{bmatrix} \text{ Where: } \mathbf{Z} \sim N(\boldsymbol{\mu}_z, \boldsymbol{\Sigma}_z), \text{ where: } \boldsymbol{\mu}_z = \begin{bmatrix} \mu_{X_1} \\ \mu_{X_2} \\ \mu_{Y_1} \\ \mu_{Y_2} \end{bmatrix}, \text{ and}$$

$$\boldsymbol{\Sigma}_z = \begin{bmatrix} \sigma_{X_1}^2 & \rho_{X_1 X_2} \sigma_{X_1} \sigma_{X_2} & \rho_{X_1 Y_1} \sigma_{X_1} \sigma_{Y_1} & \rho_{X_1 Y_2} \sigma_{X_1} \sigma_{Y_2} \\ \rho_{X_2 X_1} \sigma_{X_2} \sigma_{X_1} & \sigma_{X_2}^2 & \rho_{X_2 Y_1} \sigma_{X_2} \sigma_{Y_1} & \rho_{X_2 Y_2} \sigma_{X_2} \sigma_{Y_2} \\ \rho_{Y_1 X_1} \sigma_{Y_1} \sigma_{X_1} & \rho_{Y_1 X_2} \sigma_{Y_1} \sigma_{X_2} & \sigma_{Y_1}^2 & \rho_{Y_1 Y_2} \sigma_{Y_1} \sigma_{Y_2} \\ \rho_{Y_2 X_1} \sigma_{Y_2} \sigma_{X_1} & \rho_{Y_2 X_2} \sigma_{Y_2} \sigma_{X_2} & \rho_{Y_2 Y_1} \sigma_{Y_2} \sigma_{Y_1} & \sigma_{Y_2}^2 \end{bmatrix}$$

Now, if we need to find Vol when collect on only one or a subset of the random variables from the vector \mathbf{Z} , let us say for example on attribute X_1 , we will first need to partition the vector \mathbf{Z} as follows:

$$\mathbf{Z} = \begin{bmatrix} \mathbf{Z}_1 \\ \mathbf{Z}_2 \end{bmatrix} = \begin{bmatrix} X_2 \\ Y_1 \\ Y_2 \\ X_1 \end{bmatrix} \text{ Where: } \mathbf{Z}_1 = \begin{bmatrix} X_2 \\ Y_1 \\ Y_2 \end{bmatrix}, \mathbf{Z}_2 = X_1$$

So the mean becomes:

$$\boldsymbol{\mu}_z = \begin{bmatrix} \boldsymbol{\mu}_1 \\ \mu_2 \end{bmatrix} \text{ Where: } \boldsymbol{\mu}_1 = \begin{bmatrix} \mu_{X_2} \\ \mu_{Y_1} \\ \mu_{Y_2} \end{bmatrix}, \text{ and } \mu_2 = \mu_{X_1}$$

To find the conditional covariance matrix, we follow Schur's complement method (Sheng et al. 2008). Detailed derivation is shown in the appendix. Therefore, we now have the joint probability density function for random attributes X_2, Y_1, Y_2 , conditional on X_1 . Notice that while we only collect information on X_1 in this example for simple illustration, the same method can be used to collect information on any subgroup of the random variables. Next, we follow the same methods shown earlier when calculating Vol to find the attribute-wise Vol . A more involved example will be shown in a later section involving the selection decision between 3 vehicles with some level of autonomy, and the ideal strategy for information collection in that scenario.

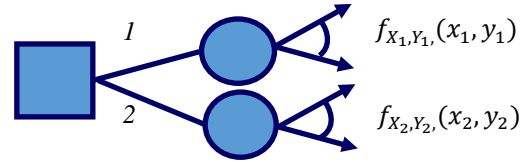


Figure 11. Notional example on two random alternatives

4. FACTORS AFFECTING Vol IN MULTI ATTRIBUTE SCENARIOS

5.1. Complement vs. Substitute attributes:

Scaling constants, k_i , measure the relative disinclination of a decision maker to trade off an attribute for improvement in other attributes. Qualitatively, we can say n attributes are complements when: $\sum_{i=1}^n k_i < 1$. In which case the normalizing constant, $K > 0$. And they are substitutes when $\sum_{i=1}^n k_i > 1$, in which case $-1 < K < 0$.

5.2. Attribute preference order:

We will investigate here the effect of the attributes' preference order on the full-attribute Vol . Let us start by recreating the results shown in Figure (9), but when attribute Y has less-is-better preference order, keeping all other inputs the same. The results are shown in Figure (12). We notice the opposite trend (increasing) of Vol as ρ increases from -1 to +1. This result is robust against changing the attributes from complements to substitute, or vice versa.

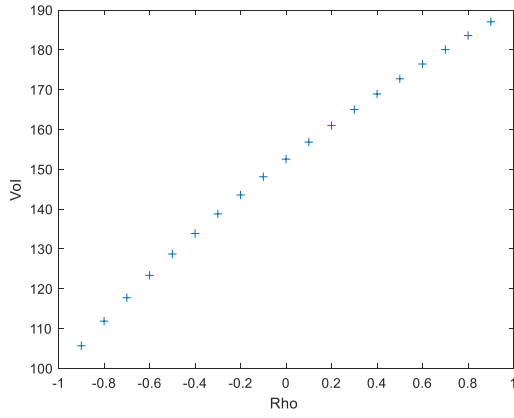


Figure 12. Vol for the example in Figure (2) when attributes are complements and involve the same preference order.

5.3. Decision maker's risk tolerance:

Here we investigate the effect of risk tolerance value for the attributes (R_i). We know that the smaller the risk tolerance, the more concave the utility function and the more risk averse the DM is. Therefore, we reduce the constants in the same example in Figure (2) to the following values and measure how that affects Vol : $R_x = 45$, $R_y = 0.25$, $R_c = 200$. One would expect that the Vol be always higher for more risk aversion. However, the results show that Vol is only higher in the region with negative correlation, and is actually lower in most of the region with positive correlation between the two random attributes. This resulted in the range between $Vol_{max, \rho=-1}$ and $Vol_{min, \rho=+1}$ becoming wider, in this particular case. Some exact values are shown in Table (3). In fact, we notice that the Vol has increased even at $\rho = 0$. The value for ρ with almost no change in Vol was at $\rho = 0.3$. This is the same value from Figure (10) with attribute-wise analysis of Vol , which had the lowest Vol when collecting information on X .

Table 3: Comparison between $Vol_{more\ aversion}$ and $Vol_{less\ aversion}$ over some ρ values (attributes with opposite preference order)

ρ	-0.9	-0.5	0	+0.5	+0.9
$Vol_{more\ aversion}$	218	206	188	165	141
$Vol_{less\ aversion}$	208	199	185	168	151
Difference	4.5%	3.5%	1.7%	-1.4%	-6.3%

Notice here that this observation occurs only when the attributes are of opposite preference order. If we run the same analysis but with attributes having the same preference order, we find that Vol increases over the full range of correlation coefficient ρ , for a more risk averse DM. The results are shown in Table (4).

Table 4: Comparison between $Vol_{more\ aversion}$ and $Vol_{less\ aversion}$ over some ρ values (attributes with same preference order)

ρ	-0.9	-0.5	0	+0.5	+0.9
$Vol_{more\ aversion}$	122	148	173	192	205
$Vol_{less\ aversion}$	106	129	153	173	187
Difference	15.6%	15.1%	13.2%	11.2%	9.8%

5.4. Attribute-wise mean, variance and preference order:

Here we investigate the factor(s) affecting the minimum value for attribute-wise Vol , let us call it Vol_{AWmin} in Figure (10). We know that increasing σ_x from 10 to 30 and reducing σ_x to 0.1 caused the notch in the Vol curve to disappear. The reason is that uncertainty now is caused more by X than Y . So there is a benefit from collecting information on X regardless of the correlation between X and Y . To confirm this theory, let us reduce σ_x to $\sigma_x = 1$ and keep $\sigma_y = 0.2$. That causes Vol_{AWmin} to be centered at $\rho = 0$ and its value then is very close to 0, to be precise $Vol_{AWmin} = 0.12$. We can also notice the wide range for Vol where the maximum value in this case is $Vol_{AWmax} = 166.7$. The reason is that uncertainty now is almost fully caused by Y attribute and, therefore, the value of collecting information on attribute X will be highly dependent on the correlation between X and Y . In fact, increasing the variance of attribute Y does not change the location of Vol_{AWmin} with respect to ρ . Instead, it only changes the range of Vol by increasing Vol_{AWmax} , here $Vol_{AWmax} = 224.7$.

It is important to note that attributes means (μ_{xa} and μ_{xb} , or in this case x_b , since option B is deterministic in this example) does not affect this trend, as long as the ratio of the two means is the same. Another important note to make here is the effect of preference order on attribute-wise Vol . While we showed previously that the “Full-attribute” Vol trend changes when the attributes have same preference order versus opposite preference order, in the case of “attribute-wise” information, the non-monotonic trend remains the same.

We also notice that changing the variance for attribute X is changing the location of the Vol_{AWmin} only in the region of positive correlation between X and Y (in the case when collecting information on X and X involves less-is better preference). Therefore, if we collect information on X , and X has a more-is-better preference order, we notice that the Vol_{AWmin} is now in the region of negative correlation coefficient between X and Y . To confirm, we overlay the “full-attribute” and “attribute-wise” Vol in this case on the same graph. The results are shown in Figure (13), which confirm our observation. This result has important implications on design and information collection strategies. The results can help decide, based on the preference order of both attributes and their variances, which attribute to collect information on. We summarize the previous results regarding the location of Vol_{AWmin} in Figure (14). We should note that these guidelines apply to the cases of 2-action decisions with one random alternative only.

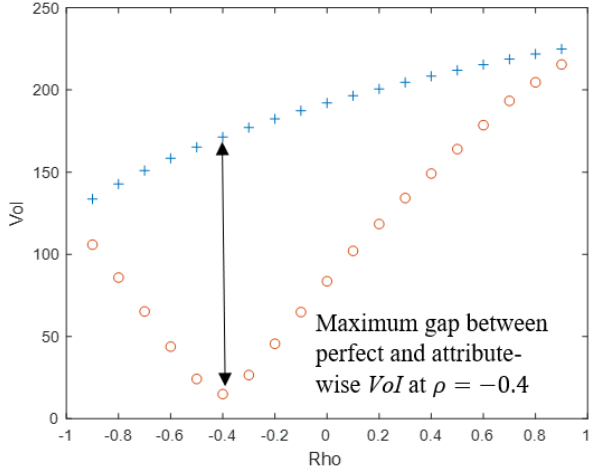


Figure 13. Difference between full-attribute (+) and attribute-wise (o) Vol (when X preference is more-is-better).

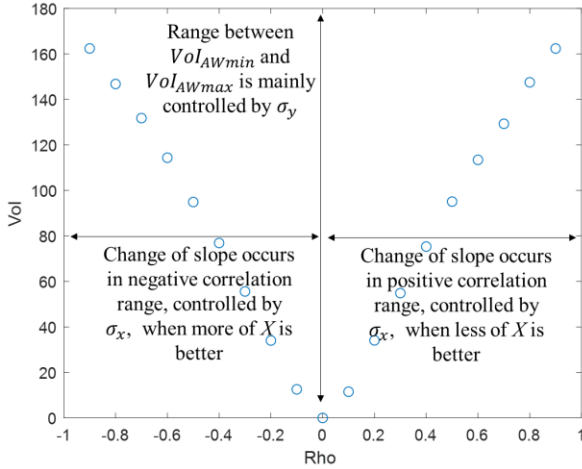


Figure 14. Location diagram and controlling factors for the Vol_{AWmin} in decision problem in Figure (2)

5. CASE STUDY: DECISIONS INVOLVING AUTONOMOUS VEHICLES

5.1. Framing the decision problem

In this section, we will apply our methods on an example decision problem involving the selection of the best vehicle platform with some level of autonomy, for a given application, and the best strategy for collecting information to mitigate the decision uncertainties. Autonomous vehicles find applications in delivery, rescue, exploration, farming, hazard disposal and many others. It should be noted that while the focus of this example is on autonomous ground vehicles, the same methodology can be used for any autonomous system in general.

Prior art has investigated intelligent vehicles mobility with respect to selecting and optimizing a certain level of autonomy (Yang et al, 2017 and Ort et al, 2018). However, the decision maker's preferences will vary based on the mission type and operating conditions. Our method provides an analytical

framework for vehicle platform selection that maximizes the utility of the decision maker under a given scenario, given the trafficability of the terrain and the intelligence and communication mix. Let us assume we have the decision in Figure (15), where a decision maker needs to select the best platform design among vehicles 1, 2 and 3, for a given operation or mission. Clearly each different mission will require different scales of the attributes tradeoff, as reflected in the scaling constants. Therefore, the alternative that maximizes the designer's utility in one specific operation will not necessarily be the best alternative in a different one. The three vehicles are to be evaluated based on three attributes: time (T) to traverse a specific terrain, trafficable percent area (A) for the vehicle on that specific terrain, and cost (c) of each vehicle. Details of the three vehicles are shown in Table (5).

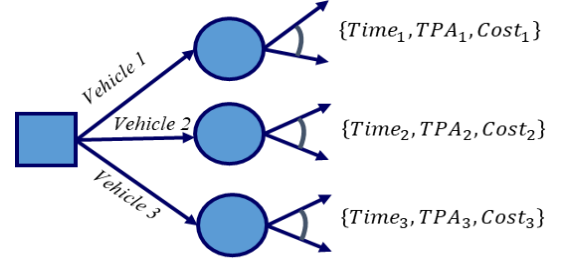


Figure 15. Example autonomous vehicles decision example with three random alternatives.

Table 5: Vehicles operation mode in the case study with corresponding attributes and uncertainties

Vehicle	Operation Mode	Time (T) (S)	TPA (A) (%)	Cost (\$)
1	Manual	100	$N(0.50, (0.3)^2)$	200
2	Tele-operated	$N(120, (30)^2)$	$N(0.65, (0.3)^2)$	350
3	Fully Autonomous	100	$N(0.65, (0.1)^2)$	800

Therefore, we have four random variables in this decision problem that are jointly distributed with a multivariate normal distribution. The correlation matrix is shown in Table (6), where we assume $\rho_{ats} = -0.7$, $\rho_{at} = -0.4$ and ρ_a is selected from the set $\{0, 0.1, \dots, 0.9\}$ to investigate its effect on Vol . The correlation between time and TPA, whether in the same alternative (ρ_{ats}) or across alternatives (ρ_{at}) is chosen to be negative, since the more trafficable percent area a vehicle can transverse on a terrain, the less time it will take to go from point A to point B on that terrain. It is also possible that for certain vehicles TPA is at the expense of speed and hence increased time, but when considering a given class of vehicles a negative correlation could be expected. Also, an increase in the TPA for one vehicle on a terrain might imply a more trafficable terrain in general, which should also be the case (to some degree) for other vehicles, hence the positive correlation region for ρ_a across vehicles. These input assumptions can be validated using simulation or actual testing.

Table 6: Correlation matrix for the 4 jointly distributed random variables in the case study

	T_2	A_1	A_2	A_3
--	-------	-------	-------	-------

T_2	I	ρ_{at}	ρ_{ats}	ρ_a
A_1	ρ_{at}	I	ρ_a	ρ_a
A_2	ρ_{ats}	ρ_a	I	ρ_a
A_3	ρ_{at}	ρ_y	ρ_a	I

In this example, we considered the time to traverse the terrain as a function of communication latency only for similar vehicle platforms. The latency is defined as the delay in communicating control actions or sensor location between a robotic vehicle and an operator, or response delay and information delay as defined by Allender, (2017). Temporal latency is a major contributor to human robot interaction (HRI) as reported by NATO (2007), which is the reason we assume vehicles 2 and 3 to have time as random variable (uncertain performance over time), with relatively higher variance for the vehicle that completely rely on tele-operation for control and sensing. All vehicles clearly encounter uncertainty over the terrain elevation, obstacles and soil type, with relatively better performance for robotic vehicles (tele-operated or fully autonomous), as they tend to withstand more uneven terrains and surfaces. We will assume the following RONS and constants in this study:

$$\begin{aligned}
RON_t &= [45s, 180s], RON_a = [10\%, 100\%] \\
RON_c &= [\$100k, \$1,000k] \\
\text{Risk tolerance factors are as follows:} \\
Rx &= 90, Ry = 0.5, Rc = 400 \\
\text{Scaling constants are as follows:} \\
k_x &= 0.2, k_y = 0.3, k_c = 0.1
\end{aligned}$$

5.2. Intelligence, communication and information.

The main goal is to find the best strategy in mitigating the uncertainties in autonomous vehicles platforms and terrains. *VoI* methods can help us in deciding whether collecting information on one attribute is better than the other, given the correlation level between the attributes and the parameters for their uncertainties. There is an increase in the amount of research on new methods for terrain remote sensing, optimal communication and bandwidth networks and other related topics in robotic and autonomous vehicles. These methods can all be considered different methods for collecting information and mitigating uncertainties in similar scenarios. Examples include the use of unmanned aerial vehicles (UAV) and drones to survey an area for obstacles and surface roughness, or the use of satellites for imaging and communications (Lucieer and Harwin, 2012 and Rivard et al, 2014). Also, prior research have looked into modeling of a given terrain, where statistical models for a terrain elevation profiles can be created, like the work of Chaika et al (2004) and Lamb et al (2007). Clearly all that comes at a cost. The cost needs to be compared to the cost of increasing the vehicle's "intelligence" through adding sensors and computational power for faster and more adaptable operation by the vehicle to its surroundings.

Results and Analysis:

First, we need to calculate the utility of each vehicle without information to compare which vehicle has higher utility. We find:

$$\begin{aligned}
E[U(vehicle_1)] &= 0.6116 \\
E[U(vehicle_2)] &= 0.6199 \\
E[U(vehicle_3)] &= 0.6133
\end{aligned}$$

The tele-operated platform has relatively higher utility than the other two vehicles. We intentionally selected the input parameters so the three vehicle have similar expected utility for illustration purposes, because that is when the *VoI* is at the highest level. If we have the options to collect information on the uncertainties in vehicles' performance, we first collect information to mitigate the uncertainty over time taken for vehicle 2, T_2 . Using the methods found earlier, we will find the results as shown in Figure (16). Since we have the correlation coefficient in this scenario between time and TPA of vehicle 2 to be $\rho_{ats} = -0.7$, then the attribute-wise value of information here is $VoI = 206$. Now, let us assume we collect information on the TPA of vehicle 2, A_2 . Not only do we reduce the uncertainty over the performance of vehicle 2, but also we gain information for the TPA of vehicles 1 and 3 because of the correlation between the TPA attributes across the three vehicles (ρ_a). We calculate the attribute-wise *VoI* in this case with the same method. The results are shown in Figure (17). We notice here that: $VoI < 206$ in the range: $0 < \rho_a < 0.8$. We conclude that collecting information on the time (or speed over the given terrain) of vehicle 2 will have more value, in this particular scenario, than collecting information on the TPA, for any level of correlation between TPA of the three vehicles below $\rho_a = 0.8$. Attribute-wise *VoI* study can, therefore, help identify the best strategy to collecting information in the presence of uncertainty.

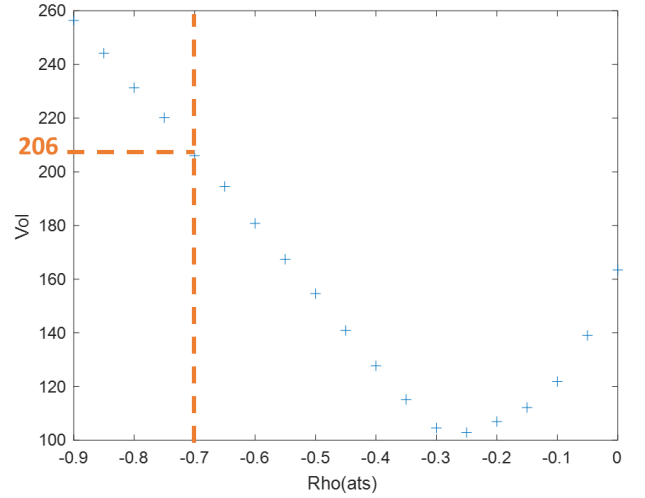


Figure 16. Attribute-wise *VoI* against the correlation between time and TPA in vehicle 2 (ρ_{ats}), when collecting information on T_2

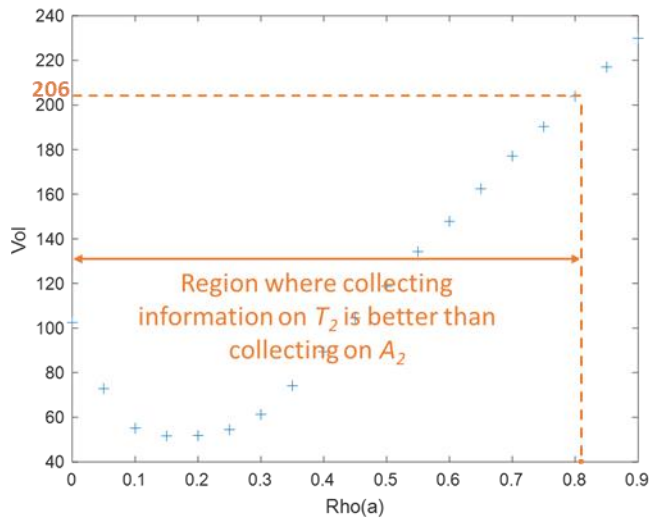


Figure 17. Attribute-wise VoI , against the correlation across the TPA of the 3 vehicles (ρ_a), when collecting information on A_2

6. CONCLUSIONS

In this paper we provided analytical and numerical methods to calculate the value of information (VoI) in multiattribute decisions under uncertainty, and when the decision maker exhibits some level of risk aversion. We validated our methods against Monte Carlo Simulation (MCS) methods and showed that the proposed methods are superior in computation time and accuracy to MCS. We also introduced a new measure for VoI called “attribute-wise VoI ” where we measure the value of collecting information on only one or a subgroup of the random variables in a decision. The main results were then summarized in a set of guidelines to show the main factors affecting VoI in multiattribute decisions. These guidelines can help decision makers (such as designers, operational planner or acquisition managers) in making good decisions under uncertainties that maximize their utility, and to plan the best information collection strategy to mitigate the uncertainties. We showed our methods in examples involving decisions on ground vehicles with some level of autonomy and uncertain performance. The results show that collecting information on one variable or the other is strictly dependent on the decision scenario and its unique inputs.

Future extension of this work is to analyze the cases when the data source is not perfect (imperfect information) and, therefore, Bayesian statistics methods should be used to draw conclusions on the posterior distribution of the unknown parameters, given a prior belief. The literature is limited in analyzing the effect of imperfect information in the case of multiattribute problems. Another extension is to conduct analysis for the scenarios when the uncertainties over the random attributes do not follow a normal distribution. While we envision that the recommendations will hold for most distributions, it is possible that certain corrections need to be made in particular cases. Lastly, Since our methods allow for automating the decision making process, one promising extension is to demonstrate the methods we found on decision

making of autonomous vehicles for instantaneous scenarios such as vehicle sensing and tracking.

ACKNOWLEDGMENTS

We acknowledge the support from the Automotive Research Center at the University of Michigan in conjunction with the US Army Tank Automotive Research, Development and Engineering Center.

REFERENCES

- [1] Allender, L., Edited: Jentsch, Florian. Human-Robot Interactions in Future Military Operations. CRC Press, 2016.
- [2] Bickel, J. E. "The Relationship between Perfect and Imperfect Information in a Two-Action Risk-Sensitive Problem." *Decision Analysis* 5, no. 3 (2008): 116-128.
- [3] Brodtkorb, P. "Evaluating Nearly Singular Multinomial Expectations with Application to Wave Distributions". *Methodology and Computing in Applied Probability*, (2006) 8(1), 65–91. doi:10.1007/s11009-006-7289-y.
- [4] Capser, S. and Nikolaidis, E., "Assessing the Value of Information for Multiple, Correlated Design Alternatives," *SAE Int. J. Commer. Veh.* (2017) 10(1).
- [5] Cardin, Michel-Alexandre, and Richard De Neufville. "A Survey Of State-Of-The-Art Methodologies And A Framework For Identifying And Valuing Flexible Design Opportunities In Engineering Systems." *Massachusetts Institute of Technology, Cambridge, MA* (2008).
- [6] Chaika, M., Gorsich, D. and Sun, T. "Some Statistical Tests in the Study of Terrain Modeling". *International Journal of Vehicle Design*, (2004) Vol 36, Nos2/3, 132-148.
- [7] Chen, Wei, Janet K. Allen, Kwok-Leung Tsui, and Farrokh Mistree. "A Procedure For Robust Design: Minimizing Variations Caused By Noise Factors And Control Factors." *Journal of Mechanical Design* 118, no. 4 (1996): 478-485.
- [8] Choi, Kyung, and Byeng Youn. "On probabilistic approaches for reliability-based design optimization (RBDO)." In *9th AIAA/ISSMO Symposium on Multidisciplinary Analysis and Optimization*, p. 5472. 2002.
- [9] De Neufville, R., and Scholtes, S. *Flexibility in engineering design*. MIT Press, 2011.
- [10] Delqu  , Philippe. "The Value of Information and Intensity of Preference." *Decision Analysis* 5, no. 3 (2008): 129-139.
- [11] Devore, J., & Berk, K. (2012). "Modern Mathematical Statistics with Applications". New York, NY: Springer New York. <https://doi.org/10.1007/978-1-4614-0391-3>
- [12] Drezner, Z. "Computation of the Bivariate Normal Integral". *Mathematics of Computation*, (1978) 32(141), 277–279. doi:10.1090/S0025-5718-1978-0461849-9.
- [13] Drezner, Z. and Wesolowsky, G. "On the Computation of the Bivariate Normal Integral", *Journal of Statistical Computation & Simulation*. (1990) No 35: 1-2, 101-107.
- [14] Evangelou, E., & Eidsvik, J. "The Value of Information for Correlated GLMS". *Journal of Statistical Planning and Inference*, (2016) 180(C), 30–48.
- [15] Fayed, H & Atiya, A. "A Novel Series Expansion For The Multivariate Normal Probability Integrals Based On Fourier Series". *Mathematics of Computation*, (2014) 83(289), 2385–2402. doi:10.1090/S0025-5718-2014-02844-5
- [16] Felder, S., Mayrhofer, T. *Medical Decision Making: A Health Economic Primer*. Springer Berlin (2017) pp.79.
- [17] Frazier, P. Powell, W. "Paradoxes in Learning and the Marginal Value of Information". *Decision Analysis*, 7(4), 378–403. (2010) <https://doi.org/10.1287/deca.1100.0190>

- [18] Genz, A. "Numerical Computation of Multivariate Normal Probabilities". *Journal of Computational and Graphical Statistics*. (1992). 1(2), 141–149.
- [19] Genz, A. "Comparison of Methods for the Computation of Multivariate Normal Probabilities". *Journal of Computing Science and Statistics*, (1993) No 25, 400–405.
- [20] Genz, A. "Numerical Computation of Rectangular Bivariate and Trivariate Normal and t Probabilities". *Statistics and Computing*, (2004) 14(3), 251–260.
- [21] Gill, Jeff. *Bayesian Methods: A Social and Behavioral Sciences Approach*. Taylor & Francis (2014) pp.581.
- [22] Howard, Ronald. "Information Value Theory" *IEEE Trans. Syst. Sci. and Cybernet.* Vol. SSC-2 No. 1 (1966): 22–26.
- [23] Keeney, Ralph L., and Howard Raiffa. *Decisions with Multiple Objectives: Preferences and Value Trade-Offs*. Cambridge university press, 1993.
- [24] Keeney, Ralph. "The Art of Assessing Multiattribute Utility Functions" *Organizational Behavior and Human Performance* Vol. 19 (1977) 267–310.
- [25] Keisler, Jeffrey. Collier, Zachary. Chu, Eric. Sinatra, Nina. Linkov, Igor. "Value of Information Analysis: The State of Application" *Envir. Sys. Dec.* Vol. 34 No. 1 (2014): 3–23.
- [26] Lamb, D., Reid, A., Truong, N., Weller, J. "Terrain Validation and Enhancements for a Virtual Proving Ground". *STAR*, (2007) 45(5). Retrieved from <http://search.proquest.com/docview/21543983/>
- [27] Liang, Jinghong, Zissimos P. Mourelatos, and Efstratios Nikolaidis. "A Single-Loop Approach for System Reliability-Based Design Optimization." *Journal of Mechanical Design* 129, no. 12 (2007): 1215–1224.
- [28] Lucieer, A. and Harwin, S. "Assessing the Accuracy of Georeferenced Point Clouds Produced via Multi-View Stereopsis from Unmanned Aerial Vehicle (UAV) Imagery". *Remote Sensing*, (2012) 4(6), 1573–1599.
- [29] Malak, Richard. Aughenbaugh, Jason. Paredis, Christiaan. "Multi-attribute Utility Analysis in Set-Based Conceptual Design" *Computer-Aided Design* Vol. 41 (2009) 214–227.
- [30] Miwa, T., Hayter, A., & Kuriki, S. "The Evaluation Of General Non-Centred Orthant Probabilities". *Journal of the Royal Statistical Society Series B-Statistical Methodology* (2003) 65, 223–234.
- [31] Mourelatos, Zissimos P., and Jinghong Liang. "A Methodology for Trading-Off Performance and Robustness under Uncertainty." *Journal of Mechanical Design* 128, no. 4 (2006): 856–863.
- [32] Nannapaneni, Saideep, Zhen Hu, and Sankaran Mahadevan. "Uncertainty Quantification in Reliability Estimation with Limit State Surrogates." *Structural and Multidisciplinary Optimization* 54, no. 6 (2016): 1509–1526.
- [33] NATO. RTO Human Factors and Medicine Panel Task Group (HFM-078/TG-017). *Uninhabited Military Vehicles (UMVs): Human Factors Issues in Augmenting the Force*. RTO Technical Report (2007) (RTO-TR-078), retrieved from: www.dtic.mil/dtic/tr/fulltext/u2/a475047.pdf.
- [34] Navidi, William. *Statistics for Engineers and Scientists*, McGraw Hill Education, 929 pages, (2015). ISBN 978-0-07-340133-1.
- [35] Olson, J & Weissfeld, L. "Approximation of Certain Multivariate Integrals". *Statistics & Probability Letters*. (1991). No 11, 309–317.
- [36] Ort, T. Paull, L. and Rus, D. "Autonomous Vehicle Navigation in Rural Environments Without Detailed Prior Maps". *ICRA* (2018). 2040–2047. 10.1109/ICRA.2018.8460519.
- [37] Panchal, Jitesh. Paredis, Christiaan. Allen, Janet. Mistree, Farrokh. "Managing Design-Process Complexity: A Value of Information Based Approach for Scale and Decision Decoupling" *Journ. Comp. Info. Sci. in Eng.* Vol.9 (2009).
- [38] Pandey, M. "An Effective Approximation To Evaluate Multinormal Integrals". *Structural Safety*, (1998) 20(1), 51–67. doi:10.1016/S0167-4730(97)00023-4
- [39] Pearson, K. "Mathematical Contributions to the Theory of Evolution. VII. On the Correlation of Characters not Quantitatively Measurable". *Philosophical Transactions of the Royal Society of London. Series A, Containing Papers of a Mathematical or Physical Character* (1896–1934), 195(262), 1–405. doi:10.1098/rsta.1900.0022.
- [40] Rivard, Lambert, and Carla Hehner-Rivard. *Complex Terrain Mapping: Integrated Use of Stereo Air Photos and Satellite Images*. Springer, 2014.
- [41] Seidl, T., Enderle, J., Vöcking, B., Alt, H., Dietzfelbinger, M., Reischuk, R., Scheideler, C., et al. "Binary Search. Algorithms Unplugged" (pp. 5–11). Berlin, Heidelberg: Springer Berlin Heidelberg (2011). doi:10.1007/978-3-642-15328-0.
- [42] Shampine, L. "Matlab program for quadrature in 2D". *Applied Mathematics and Computation*, (2008) 202(1), 266–274. doi:10.1016/j.amc.2008.02.012.
- [43] Sheng, X., & Chen, G. "Some Generalized Inverses of Partition Matrix and Quotient Identity of Generalized Schur Complement". *Applied Mathematics and Computation*, (2008) 196(1), 174–184. <https://doi.org/10.1016/j.amc.2007.05.050>
- [44] Somerville, P. "Numerical Computation of Multivariate Normal and Multivariate-t Probabilities over Convex Regions". *Journal of Computational and Graphical Statistics*, (1998). 7(4), 529–544. doi:10.1080/10618600.1998.10474793
- [45] Strong, Mark and Oakley, Jeremy E. "An Efficient Method for Computing Single Parameter Partial Expected Value of Perfect Information" *Med. Dec. Making*. Vol.33 (2013) 755–766
- [46] Strong, Mark. Oakley, Jeremy E. Brennan, Alan. "Estimating Multiparameter Partial Expected Value of Perfect information from a Probabilistic Sensitivity Analysis Example: A Nonparametric Regression Approach" *Med. Dec. Making*. Vol. 34 (2014) 311–326.
- [47] Sun, Zhengwei, and Ali E. Abbas. "On The Sensitivity of the Value of Information to Risk Aversion in Two-Action Decision Problems." *Environment Systems and Decisions* 34, no. 1 (2014): 24–37.
- [48] Wijayarathna, Kasun P., and Vinayak V. Dixit. "Impact of Information on Risk Attitudes: Implications on Valuation of Reliability and Information." *Journal of choice modelling* 20 (2016): 16–34.
- [49] Xia, Yuanpu, Ziming Xiong, Xin Dong, and Hao Lu. "Risk Assessment and Decision-Making under Uncertainty in Tunnel and Underground Engineering." *Entropy* 19, no. 10 (2017): 549.
- [50] Yang, Shun, Wenshuo Wang, Chang Liu, Weiwen Deng, and J. Karl Hedrick. "Feature Analysis and Selection for Training an End-To-End Autonomous Vehicle Controller Using Deep Learning Approach." In *Intelligent Vehicles Symposium (IV)*, 2017 IEEE, pp. 1033–1038. IEEE, 2017.
- [51] Zan, Kun, and J. Eric Bickel. "Components of Portfolio Value of Information." *Decision Analysis* 10, no. 2 (2013): 171–185.
- [52] Zhou, Jianhua, and Andrzej S. Nowak. "Integration Formulas to Evaluate Functions of Random Variables." *Structural safety* 5, no. 4 (1988): 267–284.

APPENDIX

Derivation of “Full-attribute” VoI in Equation (20):

$$E[U(V)] = E[U(V_{EU(A)>EU(B)})] + E[U(V_{EU(B)>EU(A)})]$$

Where:

$$\begin{aligned} E[U(V_{EU(A)>EU(B)})] &= \iint_D \frac{1}{K} [(Kk_x U(X_a) + 1)(Kk_y U(Y_a) + 1)(Kk_c U(c_a + V) + 1) - 1] pdf dx dy \\ &= \frac{(Kk_c U(c_a + V) + 1)}{K} \iint_D (Kk_x U(X_a) + 1)(Kk_y U(Y_a) + 1) pdf dx dy \\ &= \frac{1}{K} \iint_D pdf dx dy \end{aligned}$$

$$E[U(V_{EU(A)>EU(B)})] = -\frac{Q_1}{K} + \frac{(Kk_c U(c_a + V) + 1)}{K} * Q_2$$

Where:

$$Q_1 = \iint_{-\infty}^{f(x)x_{ymin}} pdf dx dy$$

$$Q_2 = \iint_{-\infty}^{f(x)x_{ymin}} (Kk_x U(X_a) + 1)(Kk_y U(Y_a) + 1) pdf dx dy = \iint_{-\infty}^{f(x)x_{ymin}} \gamma_a * pdf dx dy$$

$$E[U(V)] = -\frac{Q_1}{K} + \frac{(Kk_c U(c_a + V) + 1)}{K} * Q_2 + \frac{(1 - Q_1)}{K} * [(\gamma_b * (Kk_c U(c_b + V) + 1)) - 1]$$

We now equate:

$$E[U(V)] = \text{Max} EU(EU_A, EU_B)$$

And solve for (V) to find:

$$V = R_c * \ln \left[\frac{\left[\left(\frac{Kk_c}{Dc} + 1 \right) (Q_2 + \gamma_b - \gamma_b Q_1) \right] - (K * \text{Max} EU) - 1}{\left[Q_2 \left(\frac{Kk_c}{Dc} \right) e^{-\frac{(c_{max}-c_a)}{R_c}} \right] + \left[(\gamma_b - \gamma_b Q_1) \left(\left(\frac{Kk_c}{Dc} \right) e^{-\frac{(c_{max}-c_a)}{R_c}} \right) \right]} \right]$$

Derivation of Conditional Covariance Matrix for the Joint MVN Using Schur Complement:

Referring to Figure (12), let us assume the correlation matrix is as follow:

	$X1$	$X2$	$Y1$	$Y2$
$X1$	1	ρ_x	$\rho_{x_1 y_1}$	$\rho_{x_1 y_2}$
$X2$	ρ_x	1	$\rho_{x_2 y_1}$	$\rho_{x_2 y_2}$
$Y1$	$\rho_{x_1 y_1}$	$\rho_{x_2 y_1}$	1	ρ_y
$Y2$	$\rho_{x_1 y_2}$	$\rho_{x_2 y_2}$	ρ_y	1

We partition the covariance matrix as:

$$\Sigma = \begin{bmatrix} \Sigma_{11} & \Sigma_{12} \\ \Sigma_{21} & \Sigma_{22} \end{bmatrix}$$

Where:

$$\Sigma_{11} = \begin{bmatrix} \sigma_{x_2}^2 & \rho_{x_2 y_1} \sigma_{x_2} \sigma_{y_1} & \rho_{x_2 y_2} \sigma_{x_2} \sigma_{y_2} \\ \rho_{x_2 y_1} \sigma_{x_2} \sigma_{y_1} & \sigma_{y_1}^2 & \rho_y \sigma_{y_1} \sigma_{y_2} \\ \rho_{x_2 y_2} \sigma_{x_2} \sigma_{y_2} & \rho_y \sigma_{y_1} \sigma_{y_2} & \sigma_{y_2}^2 \end{bmatrix}$$

We evaluate Q_1 and Q_2 using the numerical method. Notice here that γ_a is flexible where it can be modified for higher number of random attributes in the cases of three or more random variables.

Similarly:

$$\begin{aligned} E[U(V_{EU(B)>EU(A)})] &= \iint_{f(x)x_{ymin}}^{\infty} \frac{1}{K} [(Kk_x U(x_b) + 1)(Kk_y U(y_b) + 1)(Kk_c U(c_b + V) + 1) - 1] pdf dx dy \\ &= \frac{1}{K} [(Kk_x U(x_b) + 1)(Kk_y U(y_b) + 1)(Kk_c U(c_b + V) + 1) - 1] * \iint_{f(x)x_{ymin}}^{\infty} pdf dx dy \\ &= \frac{1}{K} [(Kk_x U(x_b) + 1)(Kk_y U(y_b) + 1)(Kk_c U(c_b + V) + 1) - 1] * (1 - Q_1) \\ &= \frac{(1 - Q_1)}{K} * [(\gamma_b * (Kk_c U(c_b + V) + 1)) - 1] \end{aligned}$$

We substitute Equations (A.2) and (A.3) in (A.1) to find:

And:

$$\Sigma_{12} = \begin{bmatrix} \rho_x \sigma_{x_1} \sigma_{x_2} \\ \rho_{x_1 y_1} \sigma_{x_1} \sigma_{y_1} \\ \rho_{x_1 y_2} \sigma_{x_1} \sigma_{y_2} \end{bmatrix}$$

$$\Sigma_{21} = [\rho_x \sigma_{x_1} \sigma_{x_2} \quad \rho_{x_1 y_1} \sigma_{x_1} \sigma_{y_1} \quad \rho_{x_1 y_2} \sigma_{x_1} \sigma_{y_2}]$$

$$\text{And: } \Sigma_{22} = \sigma_{x_1}^2$$

Therefore, the conditional distribution of $\mathbf{Z}_1 | \mathbf{Z}_2 = x_1$ becomes:

$$f(\mathbf{Z}_1 | \mathbf{Z}_2 = x_1) \sim N(\mu_{cond}, \Sigma_{cond})$$

Where:

$$\mu_{cond} = \mu_1 + \Sigma_{12} \Sigma_{22}^{-1} (x_1 - \mu_{x_1})$$

$$\rightarrow \mu_{cond} = \begin{bmatrix} \mu_{x_2} \\ \mu_{y_1} \\ \mu_{y_2} \end{bmatrix} + \begin{bmatrix} \rho_x \sigma_{x_1} \sigma_{x_2} \\ \rho_{x_1 y_1} \sigma_{x_1} \sigma_{y_1} \\ \rho_{x_1 y_2} \sigma_{x_1} \sigma_{y_2} \end{bmatrix} * \sigma_{x_1}^{-2} * (x_1 - \mu_{x_1})$$

$$\rightarrow \mu_{cond} = \begin{bmatrix} \mu_{X_2} + \rho_x \sigma_{x_1}^{-1} \sigma_{x_2} (x_1 - \mu_{X_1}) \\ \mu_{Y_1} + \rho_{x_1 y_1} \sigma_{x_1}^{-1} \sigma_{y_1} (x_1 - \mu_{X_1}) \\ \mu_{Y_2} + \rho_{x_1 y_2} \sigma_{x_1}^{-1} \sigma_{y_2} (x_1 - \mu_{X_1}) \end{bmatrix} \text{ And:}$$

$$\Sigma_{cond} = \Sigma_{11} - \Sigma_{12} \Sigma_{22}^{-1} \Sigma_{21}$$

$$\rightarrow \Sigma_{cond} = \begin{bmatrix} \sigma_{x_2}^2 & \rho_{x_2 y_1} \sigma_{x_2} \sigma_{y_1} & \rho_{x_2 y_2} \sigma_{x_2} \sigma_{y_2} \\ \rho_{x_2 y_1} \sigma_{x_2} \sigma_{y_1} & \sigma_{y_1}^2 & \rho_{y_1 y_2} \sigma_{y_1} \sigma_{y_2} \\ \rho_{x_2 y_2} \sigma_{x_2} \sigma_{y_2} & \rho_{y_1 y_2} \sigma_{y_1} \sigma_{y_2} & \sigma_{y_2}^2 \end{bmatrix} - \begin{bmatrix} \rho_x \sigma_{x_1} \sigma_{x_2} \\ \rho_{x_1 y_1} \sigma_{x_1} \sigma_{y_1} \\ \rho_{x_1 y_2} \sigma_{x_1} \sigma_{y_2} \end{bmatrix} * \sigma_{x_1}^{-2} * \begin{bmatrix} \rho_x \sigma_{x_1} \sigma_{x_2} & \rho_{x_1 y_1} \sigma_{x_1} \sigma_{y_1} & \rho_{x_1 y_2} \sigma_{x_1} \sigma_{y_2} \end{bmatrix}$$

$$\Sigma_{cond} = \begin{bmatrix} \sigma_{x_2}^2 & \rho_{x_2 y_1} \sigma_{x_2} \sigma_{y_1} & \rho_{x_2 y_2} \sigma_{x_2} \sigma_{y_2} \\ \rho_{x_2 y_1} \sigma_{x_2} \sigma_{y_1} & \sigma_{y_1}^2 & \rho_{y_1 y_2} \sigma_{y_1} \sigma_{y_2} \\ \rho_{x_2 y_2} \sigma_{x_2} \sigma_{y_2} & \rho_{y_1 y_2} \sigma_{y_1} \sigma_{y_2} & \sigma_{y_2}^2 \end{bmatrix} - \begin{bmatrix} \rho_x^2 \sigma_{x_2}^2 & \rho_x \rho_{x_1 y_1} \sigma_{x_2} \sigma_{y_1} & \rho_x \rho_{x_1 y_2} \sigma_{x_2} \sigma_{y_2} \\ \rho_x \rho_{x_1 y_1} \sigma_{x_2} \sigma_{y_1} & \rho_{x_1 y_1}^2 \sigma_{y_1}^2 & \rho_{x_1 y_1} \rho_{x_1 y_2} \sigma_{y_1} \sigma_{y_2} \\ \rho_x \rho_{x_1 y_2} \sigma_{x_2} \sigma_{y_2} & \rho_{x_1 y_1} \rho_{x_1 y_2} \sigma_{y_1} \sigma_{y_2} & \rho_{x_1 y_2}^2 \sigma_{y_2}^2 \end{bmatrix}$$

Figure (A.1): MCS algorithm to calculate VoI using binary search:

